Journal of Oil Palm Research Vol. 35 (1) March 2023 p. 75-85
DOI: https://doi.org/10.21894/jopr.2022.0027

A COMPARATIVE STUDY OF OIL PALM FRONDS TORREFACTION UNDER FLUE GAS AND NITROGEN ATMOSPHERES

PREMCHAND[1]; MASAHARU KOMIYAMA[1,2,3]*; AQSHA[4] and YOSHIMITSU UEMURA[2]

ABSTRACT

Oil palm fronds' (OPF) leaves and stems were torrefied under flue gas (produced by flameless burning of wood pellets) and under inert gas (N_2) atmospheres using a fixed-bed vertical tubular reactor. The flue gas consisted of N_2 (73.7-80.2 vol%), carbon dioxide (CO_2) (12.6-16.5 vol%), oxygen (O_2) (3.7-4.6 vol%), carbon monoxide (CO) (3.7-6.0 vol%) and trace amounts of hydrogen (H_2) (up to 1.15 vol%). Detailed analyses of feed and torrefied products by proximate and ultimate analyses, thermogravimetry and infrared spectroscopy indicated that in the temperature range between 200°C and 300°C, flue gas torrefaction showed enhanced oxygen removal compared to inert gas torrefaction from both feeds, resulting in solid biomass with lower oxygen content and higher energy density. The enhanced oxygen removal under flue gas atmosphere in this temperature range was prominent for hemicellulose/cellulose components and not for lignin. The effect was attributed to O_2 present in the flue gas, accelerating the decomposition of oxygen-bearing functional groups of hemicellulose/cellulose into water, CO_2 and CO. Flue gas atmosphere did not affect the volatilisation of biomass in the form of larger organic compounds such as acetic acid, furfural and phenol within the temperature range examined here.

Keywords: calorific value ratio, energy yield, flue gas atmosphere, role of lignin, torrefaction.

Received: 1 September 2021; **Accepted:** 22 March 2022; **Published online:** 27 May 2022.

INTRODUCTION

Malaysia produces a huge amount of solid waste biomass from its oil palm industry. Many studies have been conducted on the production of biofuels via thermochemical treatments from oil palm biomasses generated at milling sites, such as empty fruit bunches (EFB), palm kernel shells (PKS) and mesocarp fibres, using torrefaction (Na *et al.*, 2013; Nyakuma *et al.*, 2021; Sabil *et al.*, 2013), pyrolysis (Asadullah *et al.*, 2013; Chantanumat *et al.*, 2022) and gasification (Iovane *et al.*, 2013). However, less consideration has been given to oil palm frond (OPF) generated at plantation sites even though OPF is the main oil palm residue which makes up to 70% of total waste from the oil palm industry (Tan *et al.*, 2016) and is available throughout the year during the pruning and harvesting of the fresh fruit bunches (FFB) (Aljuboori, 2013). Despite the fact that both OPT and OPF make up the majority of the biomass waste, the OPF are either used to feed the livestock or as a mulch, *i.e.*, being left on the plantation field to improve soil properties after the pruning process, while the trunks are usually left to decay in the plantation (Kaniapan *et al.*, 2021;

[1] Chemical Engineering Department, Universiti Teknologi PETRONAS, 32610 Seri Iskandar, Perak, Malaysia.

[2] HICoE-Center for Biofuel and Biochemical Research, Institute of Self-Sustainable Building, Universiti Teknologi PETRONAS, 32610 Seri Iskandar, Perak, Malaysia.

[3] Clean Energy Research Center, University of Yamanashi, 4-3-11 Takeda, Kofu, 400-8511 Japan.

[4] Department of Chemical Engineering, Faculty of Industrial Technology, Institut Teknologi Bandung, Jl. Ganesa No.10, Bandung, Jawa Barat, 40132 Indonesia.

* *Corresponding author e-mail: masaharu.komiyama@utp.edu.my*

Poh *et al.*, 2020). This practice offers limited benefits to the oil palm industry, as OPF is lignocellulosic biomass and has a huge potential to be used as a renewable energy source (Shuit *et al.*, 2009).

To utilise lignocellulosic biomass efficiently for biofuel production, some of its drawbacks including high moisture, high volatile matter and high oxygen contents, low energy density and hydrophilic nature must be addressed (Kanaujia *et al.*, 2014; Tabakaev *et al.*, 2017). A number of thermochemical pre-treatment techniques exist to overcome these limitations and convert raw biomass into denser energy fuels with improved properties (Zhang and Zhang, 2019). Torrefaction, a slow heating process of lignocellulosic biomass at lower temperatures (200°C-300°C) under inert atmosphere, has been presented as a promising technology to upgrade biomass to solid fuel with lower O/C ratio (Brojolall and Surroop, 2022; Prins *et al.*, 2006). Torrefaction reduces the moisture content and lowers organic volatile matters and oxygen contents within the biomass resulting in the increase of carbon content and energy density of the biomass with improved grind ability and hydrophobicity (Agar *et al.*, 2012; Ibrahim *et al.*, 2013). However, the concerns of large-scale use of inert gas in the process have drawn researchers' attention to find an effective substitute. The concept of utilising industrial flue gases as torrefaction atmosphere can be an efficient way to upscale this process. This would not only replace the need of pure nitrogen (N_2) gas in the torrefaction but also would provide thermal energy necessary for torrefaction process. In light of this, several studies have been conducted for torrefaction under non-inert atmospheres [air, oxygen (O_2), carbon dioxide (CO_2) and their mixtures] and the effects of these gases on torrefaction performance have been reported (Eseltine *et al.*, 2013; Li *et al.*, 2016; 2021; Rousset *et al.*, 2012; Tran *et al.*, 2016; Uemura *et al.*, 2013). For instance, the addition of O_2 (3%-15%) in N_2 resulted in the decrease of both mass yield and energy yield (Uemura *et al.*, 2013). Torrefaction of corncob found that pure CO_2 atmosphere gives higher solid yield and better energy yield compared to pure N_2 atmosphere at 260°C (Li *et al.*, 2018).

Along with N_2, CO_2 and O_2, there are some other gases also present in flue gases in minor quantities such as carbon monoxide (CO), hydrogen (H_2) and water vapour and thus, the previous studies about utilisation of a mixture of N_2, O_2 and/or CO_2 from the cylinders may not show the same effect of real flue gas on torrefaction. In the near past, our group carried out torrefaction of EFB and OPF in the atmosphere of real combustion gas generated by burning wood pellets with the findings that flue gases from the industrial boilers can be used in the torrefaction reactor without any significant problem (Premchand *et al.*, 2020; Uemura *et al.*, 2017).

In the present study, torrefaction of OPF has been carried out under flue gas and inert (N_2) gas atmospheres in the temperature range between 200°C and 300°C. Oil palm frond was separated into frond leaves (OPFL) and frond stems (OPFS) to compare the effect of proximate compositional differences. The research gaps present are twofold: 1) torrefaction characteristics of OPF have not been well known, and 2) the mechanism of flue gas torrefaction has not been well understood for any lignocellulosic feed. The present research tried to present data for gap and tried to present new insight into possible flue gas torrefaction mechanism for gap. Findings from this research would aid in utilising a huge amount of OPF waste through the economic flue-gas torrefaction process.

MATERIALS AND METHODS

Sample Preparation

OPF were collected from an oil palm plantation in Bota, Perak, Malaysia. The fronds were washed and separated into two portions; one was the stem part (OPFS) and the other was the leaf part (OPFL). These two portions have widely differed proximate, ultimate and ash compositions to each other as listed in *Table 1*, which are expected to affect their torrefaction behaviour. Respective samples were dried at 105°C before their characterisations and torrefaction experiments.

Torrefaction Process

The reactor setup and the details of torrefaction procedure are found elsewhere (Uemura *et al.*, 2017). Briefly, the torrefaction reactor consisted of two stainless steel vertical chambers: One chamber for wood pellets combustion and the other for conducting torrefaction experiments. Torrefaction chamber was equipped with an electric heater and four thermocouples installed within the reactor at different depths of the biomass bed. Two glass condensers dipped into the ice water chiller were connected in series at the outlet of the torrefaction chamber for collecting condensable liquid products.

For inert gas torrefaction, N_2 gas was directly introduced to the torrefaction reactor from a cylinder. For flue gas torrefaction, first the wood chips placed in the combustion chamber were ignited and burnt until they reached flameless char combustion stage. Then, the flue gas from the combustion chamber was introduced into the torrefaction reactor through an air-cooled stainless-steel pipe. This way it is assured that only non-condensable gases (N_2, O_2, CO_2, CO and H_2) from the combustion chamber would enter the torrefaction chamber. Flue gas compositions at

TABLE 1. PROXIMATE, ULTIMATE, CALORIFIC VALUE, AND ASH COMPOSITIONS OF FEEDSTOCKS

Item	OPFL (wt%)	OPFS (wt%)
Proximate composition		
Moisture (wb)	6.86	5.01
Ash (db)	3.89	2.79
Volatile matter (db)	81.94	85.49
Fixed carbon (db)	14.17	11.72
Hemicellulose/cellulose (Abnisa *et al.*, 2013; Hashim *et al.*, 2011)	55	73
Lignin (Abnisa *et al.*, 2013; Hashim *et al.*, 2011)	26-27	20-22
Ultimate composition (db)		
Total carbon	47.65	44.02
Hydrogen	6.96	5.61
Nitrogen	1.68	0.52
Oxygen	39.82	47.06
Calorific value (MJ/kg)	18.02	17.39
Ash composition (db)		
Calcium	58.3	74.3
Potassium	8.8	8.9
Silicon	22.0	5.2
Magnesium	2.1	4.0
Sulphur	1.8	2.8
Phosphorus	4.1	2.4
Chlorine	0.7	0.9
Iron	0.7	0.5
Manganese	1.0	0.3

Note: wb - wet basis; db - dry basis.

the inlet of the torrefaction chamber are listed in *Table 2*, along with the outlet compositions of non-condensable product gases, for all the torrefaction runs performed here. All values presented in *Table 2* are the average over the 30-min torrefaction period (time-integrated), the procedure of which was justified since the gas compositions during the torrefaction was quite stable. The temperature of the torrefaction chamber was raised from room temperature with a heating rate of 4°C/min up to the desired temperature and kept at the temperature for 30 min. The flow rate of N_2 or flue gas to torrefaction reactor was kept at 4 L/min or 5 L/min by a mass flow controller. The temperatures of

TABLE 2. COMPOSITIONS (VOL %) OF INLET AND OUTLET GASES FROM TORREFACTION OF OPFL AND OPFS

		N_2 atmosphere						Flue gas atmosphere					
		200°C		250°C		300°C		200°C		250°C		300°C	
		Inlet	Outlet	Inlet	Outlet	Inlet	Outlet	Inlet	Outlet	Inlet	Outlet	Inlet	Outlet
OPFL	N_2	100.00	98.32	100.00	93.32	100.00	93.53	75.79	74.48	80.21	77.77	78.97	70.63
	H_2	-	0.00	-	0.00	-	0.28	1.01	0.86	0.32	0.28	1.08	1.78
	O_2	-	0.43	-	0.42	-	0.49	3.18	2.73	4.56	2.51	4.38	0.19
	CO	-	0.00	-	0.00	-	0.67	3.77	4.42	1.69	3.78	2.93	9.23
	CO_2	-	1.25	-	6.26	-	5.02	16.25	17.07	13.21	15.66	12.63	18.18
OPFS	N_2	100.00	96.20	100.00	91.27	100.00	84.53	75.51	74.07	79.18	68.79	78.28	63.56
	H_2	-	0.00	-	0.00	-	0.78	1.15	0.64	0.38	0.31	0.82	0.31
	O_2	-	0.54	-	0.48	-	1.05	2.63	2.09	2.94	0.37	4.62	0.15
	CO	-	0.38	-	0.00	-	3.46	4.22	6.02	2.94	6.50	2.62	7.94
	CO_2	-	2.88	-	8.24	-	10.18	16.49	18.99	14.56	24.03	13.66	28.03

torrefaction chamber were closely monitored using four thermocouples inserted to the various depth of the chamber. While there were certain variations of chamber temperature depending on the position, each thermocouple reading was quite stable during the torrefaction. No signs of hot spot appearance, which would indicate local combustion of samples due to O_2 in the flue gas, were observed.

Product Characterisation and Data Processing

The feed and solid products were characterised by proximate (following respective ASTM procedures), ultimate (Series II CHNS/O Analyser 2400, Perkin Elmer) and calorific value (Bomb Calorimeter Model C200, IKA Werke) analyses. Ash compositions were analysed by using X-ray fluorescence analyser (Model S8 Tiger). Surface functional groups on the feed and torrefied biomass were observed by using an Fourier transform infrared spectroscopy (FT-IR) spectrophotometer (Nicolet iS10). Thermogravimetry was carried out by using a thermogravimetric analyser (TGA) (TGA Q50, TA instruments). The water content in liquid bio-oil collected at the outlet of the torrefaction chamber was determined through a volumetric Karl Fischer titrator (Model V30) and the organic compounds in bio-oil were identified through a gas chromatography-mass spectrometer (Agilent GC-MSodel 7890A) with a column HP 5MS. The compositions of inlet flue gas and non-condensable gases from the torrefaction process were analysed by using a gas chromatography with a thermal conductivity detector (Shimadzu GC-8A) with column packings of MS-5A and Porapak Q. The liquid yield (Y_l), solid yield(Y_m), calorific value ratio (CV_{ratio}), energy yield (Y_E), CO_2 yield (Y_{CO_2}) and CO yield (Y_{CO}) were calculated by using the following Equations:

$$Y_l\,(\text{wt\%}) = \frac{m_l}{m_i} \times 100 \quad (1)$$

$$Y_m\,(\text{wt\%}) = \frac{m_f}{m_i} \times 100 \quad (2)$$

$$CV_{ratio} = \frac{CV_f}{CV_i} \times 100 \quad (3)$$

$$Y_E = Y_m \times CV_{ratio} \quad (4)$$

$$Y_{CO_2} = Y_g \times \textit{mass fraction of } CO_2 \textit{ in the inlet or outlet gas} \quad (5)$$

$$Y_{CO} = Y_g \times \textit{mass fraction of CO in the inlet or outlet gas} \quad (6)$$

where m indicates the mass of biomass and subscripts i and f denote the initial stage (before torrefaction) and the final stage (after torrefaction), respectively.

RESULTS AND DISCUSSION

Effect of Flue Gas on Torrefaction Products

Figure 1 compares the torrefaction product (gas, liquid and solid) yields in weight percentages (wt%). Overall, it shows that flue gas torrefaction (right half of the figure) gives higher amounts of liquid (bio-oil) and gaseous products combined at the cost of solid yields compared to inert-gas torrefaction (left half of the figure) at all the three temperatures examined here. Within each torrefaction atmosphere, higher temperature produces a higher amount of gas and liquid combined at the cost of solid yields. Obviously, higher temperature increases the severity of torrefaction, and the flue gas atmosphere enhances the severity as compared to the N_2 atmosphere. This trend is consistent with the previously reported observations (Onsree *et al.*, 2019; Uemura *et al.*, 2017).

First, the details of solid product which is the main objective of biomass torrefaction are examined. The effect of torrefaction atmosphere and temperature on energy yield and calorific value ratio (CV_{ratio}, a ratio of CV of each solid product to the CV of respective biomass feed, used here only for solid product) from torrefaction of OPFL and OPFS are shown in *Figure 2*. Calorific value ratio (CV_{ratio}) increases as temperature rises from 200°C to 300°C for both the biomass feed and for both the torrefaction atmospheres. As discussed above, the rise in temperature increased the severity of torrefaction which led to extensive devolatilisation of lignocellulosic biomass resulting in increased carbon content and ultimately increased the product CV (Sabil *et al.*, 2013; Uemura *et al.*, 2017). Since flue gas enhances the severity of torrefaction, as seen in *Figure 1*, CV_{ratio} for torrefied OPFL and OPFS in flue gas are always higher than that in N_2 torrefaction at all the temperatures examined here and these findings appear to be consistent with the literature (Uemura *et al.*, 2017).

The major reason for this CV_{ratio} increase is found in the proximate and ultimate compositions of the product solids listed in *Table 3*. With increasing torrefaction severity (temperature and atmosphere), fixed carbon (FC) and total carbon (C) increased whereas volatile matter (VM) and oxygen (O) contents decreased, and so did the O/C ratio. Apparently, the CV increase found in *Figure 2* is brought about by the decrease of oxygen content, with concomitant relative increase of carbon content, due to the severer torrefaction conditions (temperature and atmosphere). It is stressed that the flue gas always enhanced these tendencies compared to inert gas, N_2, at similar torrefaction temperatures. This leads to the observation that the effect of flue gas atmosphere is to volatilise more of the oxygen containing entities in the feed biomass than N_2 atmosphere.

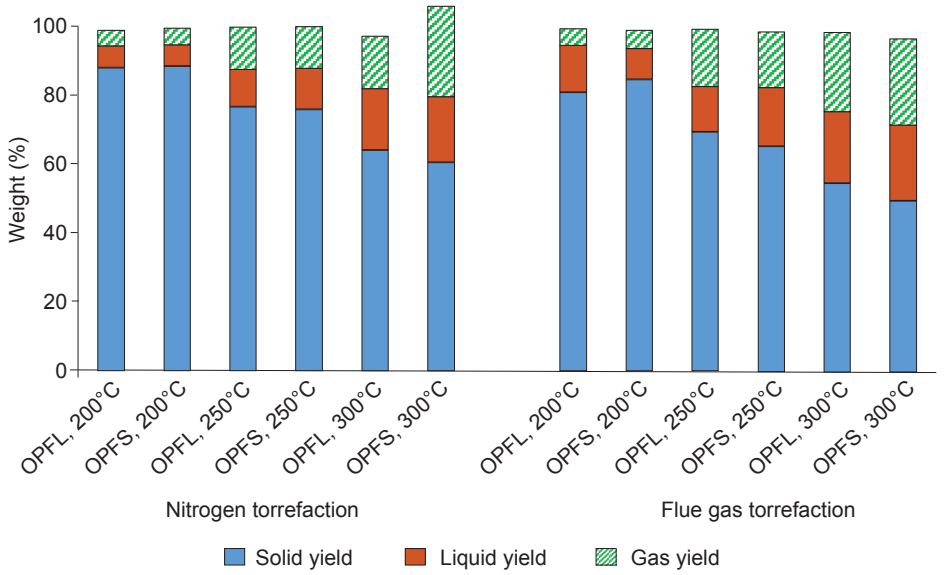

Figure 1. Yields (wt%) of solid, liquid and gas from the torrefaction of OPFL and OPFS under N_2 (left columns) and flue gas (right columns).

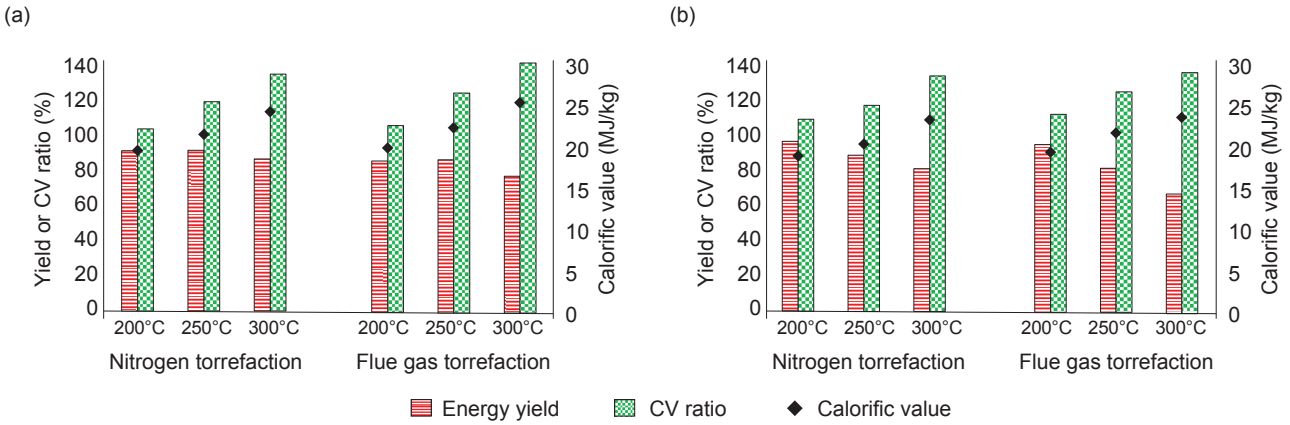

Figure 2. Calorific value, energy yield and CV ratio from the torrefaction of (a) OPFL and (b) OPFS.

TABLE 3. PROXIMATE AND ULTIMATE ANALYSES (wt%) OF RAW AND TORREFIED OPFL AND OPFS SOLIDS

			Proximate analysis				Ultimate analysis (db)					
			MC (wb)	VM (db)	Ash (db)	FC (db)	C	H	N	O	H/C	O/C
N_2 torrefaction	OPFL	200°C	1.03	77.93	5.18	16.89	50.64	5.90	1.45	36.83	0.117	0.727
		250°C	0.74	74.47	5.29	20.24	52.89	4.71	1.89	35.22	0.089	0.666
		300°C	0.64	68.28	6.82	24.90	56.87	3.41	1.95	30.95	0.060	0.544
	OPFS	200°C	0.72	80.02	3.46	16.52	45.67	4.58	0.35	45.93	0.100	1.006
		250°C	0.78	77.14	3.18	19.68	48.76	4.89	1.78	41.40	0.100	0.849
		300°C	0.77	69.60	4.27	26.13	52.51	3.86	1.71	37.64	0.074	0.717
Flue gas torrefaction	OPFL	200°C	0.72	75.75	5.31	18.94	51.74	5.87	1.78	35.30	0.113	0.682
		250°C	0.53	72.38	5.41	22.21	54.02	4.08	1.92	34.58	0.076	0.640
		300°C	0.59	66.36	7.96	25.68	59.68	3.06	1.98	27.32	0.051	0.458
	OPFS	200°C	0.64	78.41	4.38	17.21	47.59	3.74	0.22	44.06	0.079	0.926
		250°C	0.89	71.87	3.29	24.84	51.50	3.98	1.82	39.41	0.077	0.765
		300°C	0.70	67.94	4.61	27.45	55.26	3.34	1.85	34.94	0.060	0.632

Note: MC - moisture content; VM - volatile matter; FC - fixed carbon; wb - wet basis; db - dry basis.

Details of the volatilised matter, *viz.*, gas and liquid products, corroborate this observation. *Table 2* lists as-measured inlet and outlet torrefaction gas compositions. It is found in the table that the major gaseous products from torrefaction are CO_2 followed by CO (note that in this table inlet CO_2 and CO are not subtracted from the outlet CO_2 and CO). Therefore, in *Figure 3* net yields of CO_2 and CO from each torrefaction experiment is compared, along with the yields of water and organic matter collected as liquid products. Generally (with a few minor exceptions), higher temperature resulted in higher water, organic matter, CO_2, and CO yields and again, flue gas atmosphere enhanced this trend in terms of water, CO_2, and CO yields. Note that the yield of organic matter (calculated by subtracting the water weight percentage from bio-oil in total) did not change appreciably when torrefaction atmosphere is changed from inert N_2 to flue gas. Major organic matters in the bio-oil found by GC-MS analysis were acetic acid, followed by furfural, phenol and 1-hydroxy-2-propanone and these findings are consistent with previous research for the torrefaction of different biomass under inert and non-inert atmospheres (Chai *et al.*, 2021; Uemura *et al.*, 2017). Those data lead to the conclusion that flue gas atmosphere enhances the biomass volatilisation into simpler oxygen-bearing molecules such as water, CO_2, and CO but not into larger and more complex liquid organic molecules.

The Influence of O_2 and CO_2 in Flue Gas Torrefaction

Detailed product analysis in the previous section indicated that the present torrefaction eliminates oxygen from the feed, and the tendency is prominent with flue gas torrefaction compared to inert gas (N_2) torrefaction. In order to identify the components affected by flue gas torrefaction, FT-IR spectroscopy was performed on raw and torrefied solids and the obtained spectra are compared in *Figure 4a* and *4b* for OPFL and OPFS, respectively. The peak assignment was carried out following the

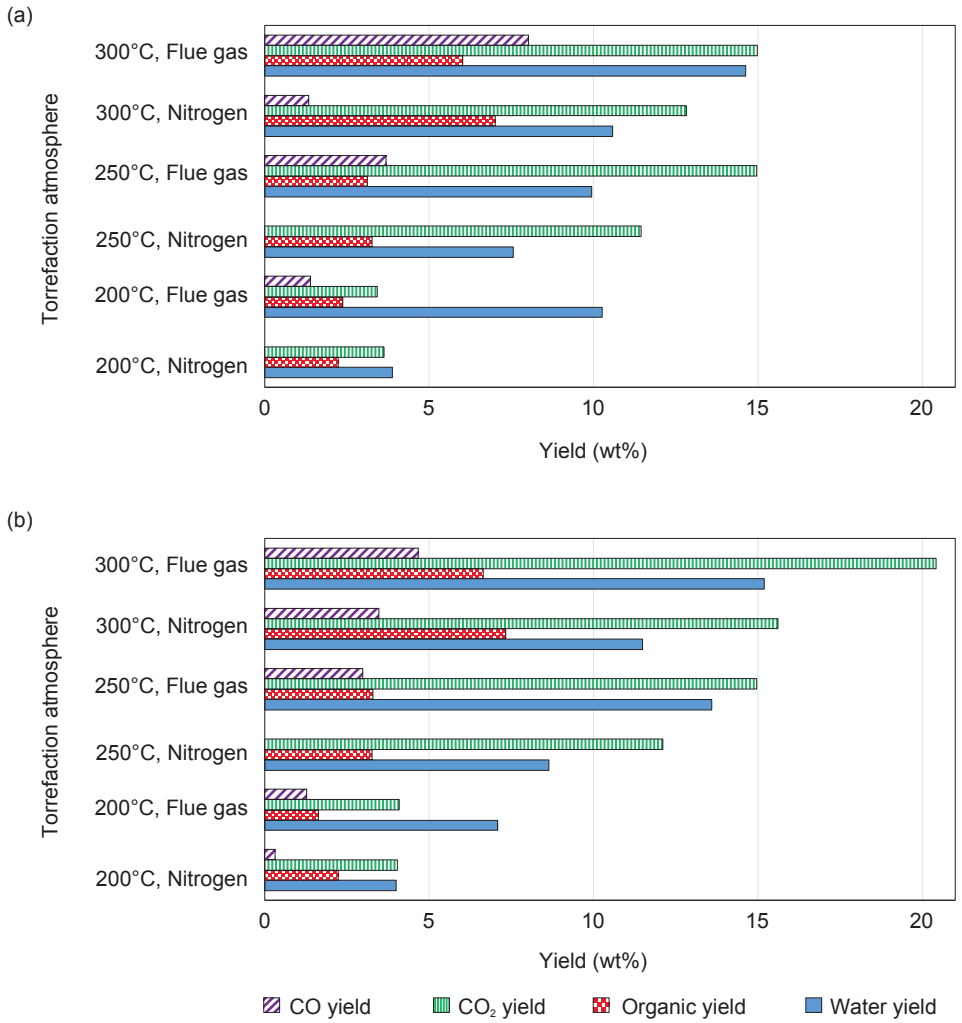

Figure 3. Yields (wt%) of water and organic compounds in bio-oil and CO_2 and CO in gaseous product from the torrefaction of (a) OPFL and (b) OPFS. Inlet CO and CO_2 have been subtracted for the respective yield calculations in the case of flue gas torrefaction.

references (Bilgic *et al.*, 2016; Hon and Shiraishi, 2001; Lv *et al.*, 2015; Matsunaga *et al.*, 1999) as listed in *Table 4*, along with their disappearance trends due to torrefaction process (last two columns).

The IR spectra of raw OPFL and OPFS (spectrum a in *Figure 4a* and *4b* consist of 13 peaks: 8 from hemicellulose/cellulose (α, β, χ, η, φ, κ, λ and μ) and five from lignin (δ, ε, ϕ, γ and ι). It is noted that many of the major peaks identified here (α, δ, ϕ, κ, λ and μ) are related to O-bearing functional groups. The most visible peak from the hemicellulose/cellulose group is C-OH in glucans or other unit sugars, which is the origin of the two major peaks α and μ as found in *Figure 4*. Their intensities decreased in torrefied samples because of dehydration, one of the major reactions in torrefaction. Similar decrease was reported by previous studies (Lv *et al.*, 2015). All other middle to low intensity peaks lost their intensities in comparison with the raw samples in a similar manner.

In addition to this major general trend, scrutiny of the IR spectra found the sub-trend of intensity losses between the two atmospheres (*Table 4*, last two columns) that can be classified into two types: Sub-trend A indicates peak intensity loss with temperature irrespective of the torrefaction atmosphere, and sub-trend B indicates peak intensity loss with temperature with apparent effect of flue gas.

Close examination of those two peaks intensity sub-trends in *Figure 4* and their breakdown listed in *Table 4* (last two columns) provides two observations: (1) all the IR peaks affected by the torrefaction atmosphere difference, *viz.*, sub-trend B, belong to hemicellulose/cellulose but not to lignin, and (2) OPFL shows very weak effect (if any) of torrefaction atmosphere compared to OPFS, as almost all of OPFL infrared peaks belong to sub-trend A. The first observation apparently indicates that flue gas as a torrefaction atmosphere enhances

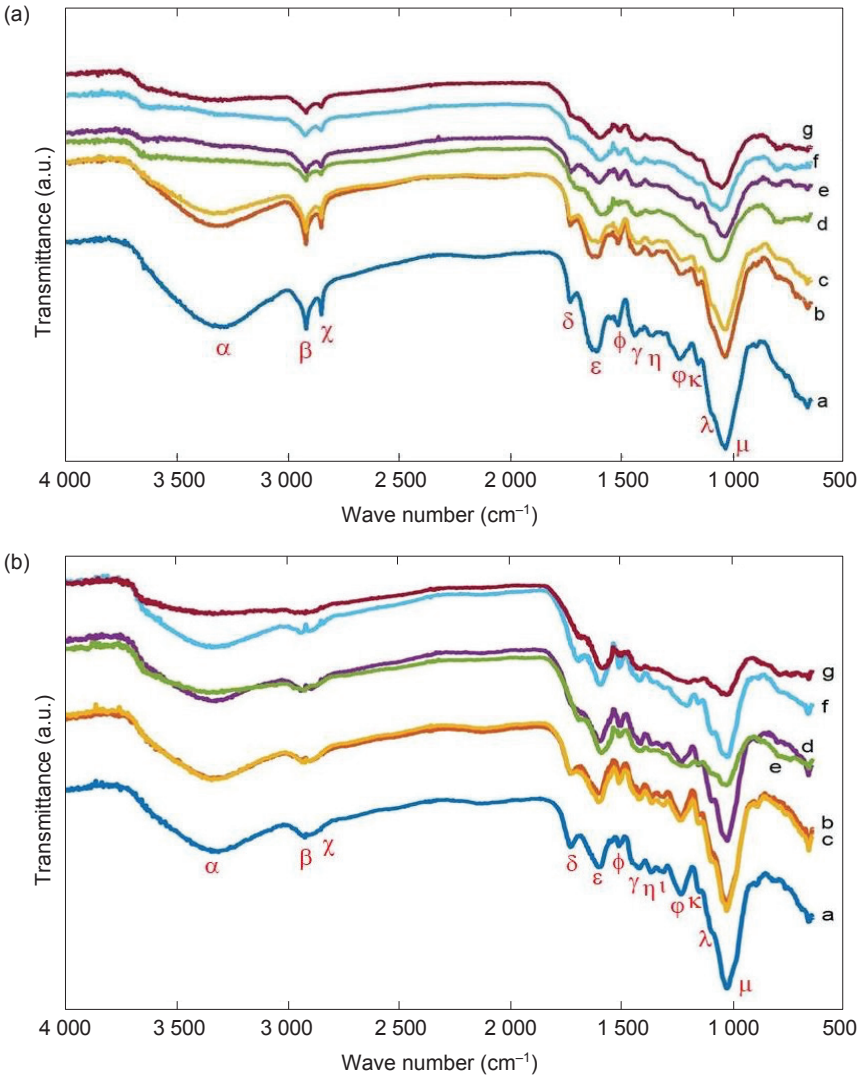

Figure 4. FT-IR spectra of OPFL (A) and OPFS (B): (a) raw, (b) torrefied under N_2 at 200°C, (c) torrefied under flue gas at 200°C, (d) torrefied under N_2 at 250°C, (e) torrefied under flue gas at 250°C, (f) torrefied under N_2 at 300°C and (g) torrefied under flue gas at 300°C. For peak assignments, see Table 4.

TABLE 4. FT-IR SPECTRA OF RAW AND TORREFIED OPFL AND OPFS

Code	Wave number (cm^{-1})		Assignment	Component*	Sub-trend**	
	OPFL	OPFS			OPFL	OPFS
α	3 316	3 316	OH stretching	HC and C	B	B
β	2 917	2 936	CH2 stretching	HC and C	A	B
χ	2 853	2 899	CH2 symmetric stretching	HC and C	A	B
δ	1 737	1 735	C=O stretch	L	A	A
ε	1 623	1 603	Aromatic skeletal	L	A	A
ϕ	1 529	1 518	Aromatic skeletal vibration	L	A	Not clear
γ	1 449	1 426	Aromatic skeletal *etc.*	L	A	A
η	1 375	1 371	CH bending	HC and C	A	B
ι	Not detected	1 320	S-ring plus G-ring condensed	L	Not detected	Not clear
φ	1 248	1 239	CH2 wagging, CH and OH deformation	HC	A	B
κ	1 167	1 162	Anti-symmetric stretching of C-O-C glycosidic linkages	HC and C	A	B
λ	1 101	1 110	CO (of COH) stretching	HC and C	A	B
μ	1 046	1 037	CO (of COH) stretching	HC and C	A	B

Note: * HC - hemicellulose; C - cellulose; L - lignin.

** Sub-trend A: peak intensity loss with temperature irrespective of the torrefaction atmosphere, sub-trend B: peak intensity loss with temperature with apparent effect of flue gas.

hemicellulose/cellulose degradation but not lignin. The second observation, then, may serve as supporting evidence of the first observation since OPFL composition is known to have much higher lignin content than OPFS (*Table 1*) (Abnisa *et al.*, 2013; Hashim *et al.*, 2011). A direct consequence of these observations is that, since lignin may play a role as a protector of hemicellulose and cellulose from thermal degradation and external chemical attack during torrefaction (Financie *et al.*, 2016; Wertz *et al.*, 2010), biomass with a higher amount of lignin content would be more tolerant to the combustion gas torrefaction. This conjecture would be natural if we recall that lignin is situated in a way to cover hemicellulose/cellulose, and if flue gas is to attack hemicellulose/cellulose it has to be done on the points where hemicellulose/cellulose is exposed or thinly covered by lignin through which flue gas penetrates to attack hemicellulose/cellulose.

The next question that may arise in the present study would be; which extra component in flue gas (mostly CO_2 and O_2, cf. *Table 2*) compared to inert atmosphere would be the cause of these flue gas torrefaction characteristics? There exist a few studies on the effect of pure CO_2 atmosphere torrefaction compared to pure N_2 atmosphere torrefaction, with mixed conclusions (Eseltine *et al.*, 2013; Howell *et al.*, 2019; Li *et al.*, 2018; Thanapal *et al.*, 2014). Eseltine *et al.* (2013) and Thanapal *et al.* (2014) compared the torrefaction of two different woody biomasses (Mesquite and Juniper) under pure N_2 and pure CO_2 atmospheres using TGA. By holding the samples at various torrefaction temperatures between 200°C and 300°C for 1 hr duration, they found that pure CO_2 atmosphere gives higher weight loss for both the samples above 240°C. Above 280°C, the weight loss difference between the two atmospheres was 3.8%-4.8% for both samples (Eseltine *et al.*, 2013). Energy retention values obtained from batch torrefaction experiments also followed similar trend. With a larger amount of batch torrefaction, however, the two atmospheres showed a difference only after 280°C for Mesquite and after 300°C for Juniper (Thanapal *et al.*, 2014). On the contrary, a study on the corncob torrefaction (Li *et al.*, 2018) reported that both pure N_2 and pure CO_2 torrefaction at 220°C resulted in the same solid yield, while at 260°C, CO_2 torrefaction showed 10.7% higher solid yield than N_2 torrefaction. Nevertheless, energy yield was better with pure CO_2 torrefaction above 260°C. This may point to the possibility that the CO_2 effect on torrefaction maybe feed dependent. More recently, Howell *et al.* (2019) reported Miscanthus torrefaction in pure N_2 and pure CO_2 using gas specific TGA calibration. They found mass yield to be independent of torrefaction atmosphere, and so is the heating value obtained from batch torrefied samples.

On the other hand, one of the present authors studied the effects of O_2 and CO_2 addition (up to 15 vol% each) in N_2 atmosphere on PKS torrefaction (Uemura *et al.*, 2013; 2015). It was found that the effects of O_2 and CO_2 addition (separately) to N_2 atmosphere became apparent at 300°C. The

increment of mass loss due to O_2 or CO_2 addition compared to pure N_2 torrefaction amounted to a few to 15% and O_2 addition removed more differential mass, 1.5 to 2.0 times as much, compared to CO_2 addition (Uemura *et al.*, 2015).

In order to examine the effect of CO_2 on the present torrefaction, TGA under pure N_2 and under simulated flue gas (20 vol% CO_2 + N_2) were compared for the present two samples. Due to the equipment limitation, no O_2 was able to be added in the simulated flue gas. The results are shown in *Figure 5*. Firstly, it is noted in the TGA profiles that OPFL experiences less weight loss compared to OPFS in the almost entire temperature range scanned here (up to 800°C), with a very minor exception in the temperature range between 100°C and 200°C. This lower weight loss of OPFL is the TGA manifestation of the torrefaction results in which OPFL produced higher solid yield (*Figure 1*) and higher CV_{ratio} compared to OPFS (*Figure 2*), as well as its lesser hemicellulose/cellulose IR peak intensity losses under flue gas torrefaction than OPFS.

When the two TGA atmospheres are compared, apparent differences are observed above 350°C for OPFS and above 500°C for OPFL. Below those temperature ranges, which includes the torrefaction temperature examined here (200°C-300°C), the addition of 20% CO_2 to pure N_2 does not seem to affect the weight loss of these biomass feeds. This could be interpreted in two ways: (1) for the present samples, the effect of CO_2 (20% in the torrefaction atmosphere) is very weak in the torrefaction temperature examined here (200°C-300°C). This interpretation is supported by the appearance of CO_2 effect at higher temperatures for both samples (*Figure 5*). (2) The weight losing process caused by the addition of CO_2 is very slow to appear in the TGA analysis with temperature ramping (not temperature holding), in other words, kinetically limited to be apparent within the TGA ramping time frame. On this point, it is noted that other TGA work is done at 100% of CO_2 concentration (Thanapal *et al.*, 2014) which would have accelerated the reaction compared to lower CO_2 concentration, and also that the CO_2-induced weight loss showing positive order on CO_2 concentration (1.7 in the case of PKS torrefaction) (Uemura *et al.*, 2015) which would indicate that higher concentration CO_2 accelerates the CO_2-related reactions. The above discussion seems to indicate that CO_2 participation with the present concentration in the flue gas (12.6%-16.5%) is weak or slow, and the present flue gas torrefaction of OPF on the enhanced solid yield decrease observed in *Figure 1* during the present flue gas torrefaction within the temperature range of 200°C-300°C would be attributed to the stronger participation of O_2. The effect of CO_2 would be more pronounced at the higher temperatures, as found in *Figure 5*, under the present conditions.

Possible Mechanism of Flue Gas Torrefaction

With all the collected data combined, it may be able to conjecture the following mechanism for the present flue gas torrefaction in the temperature range of 200°C-300°C. The O_2 in flue gas attacks O-bearing surface functional groups, extracting CO_2, CO and H_2O from terminal C=O, C-O-C, C-O and C-OH groups (*Figure 4*), resulting in lower H and O contents (*Table 3*) and thus, increasing C content (*Table 3*) and higher CV ratio (*Figure 2*) for the product solids than torrefaction under N_2. The flue gas attack appears to be mostly on hemicellulose/cellulose components of biomass (*Figure 4* and *Table 3*), indicating that lignin-rich biomass (OPFL in the present study) would be more tolerant toward flue gas as torrefaction atmosphere.

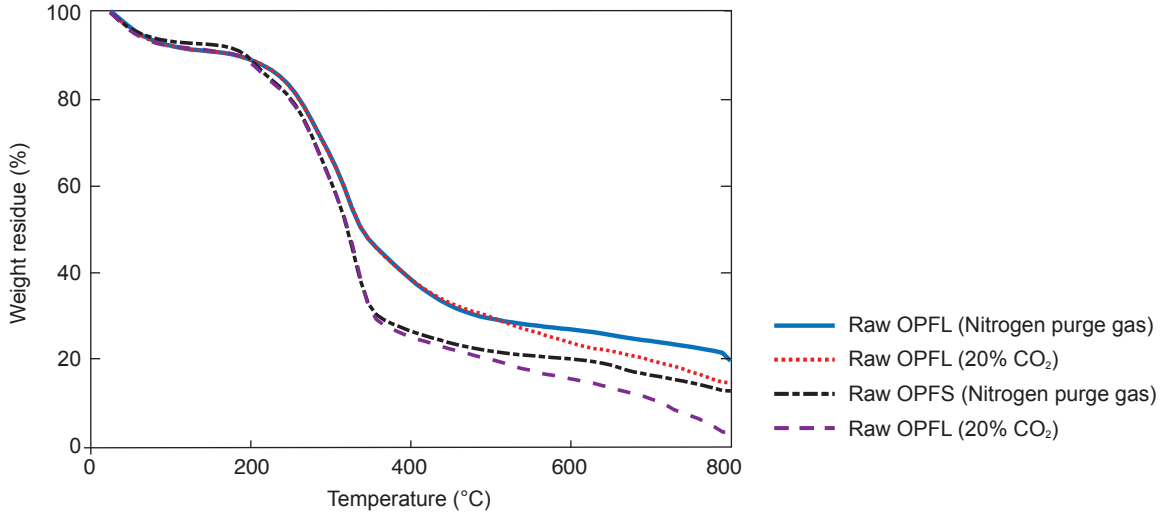

Figure 5. Weight loss profile (TGA curves) of raw OPFL and OPFS in the atmosphere of N_2 purge gas and 20% CO_2 mixed in N_2.

CONCLUSION

A comparative study of the torrefaction of OPF leaves and stems was performed under flue gas and inert N_2 atmospheres. Results indicated that flue gas atmosphere caused severer torrefaction than N_2 atmosphere, resulting in flue gas torrefied biomass producing solid products with higher calorific value ratio than N_2 torrefied ones in the temperature range of 200°C-300°C. The torrefaction severity of flue gas atmosphere is attributed to the presence of O_2 in the gas, causing increased removal of O from the feed compared to the torrefaction in the N_2 atmosphere. Lignin component appears to retard this flue gas attack on hemicellulose/cellulose components of biomass, as lignin-rich biomass (OPFL in the present study) would be more tolerant to the use of flue gas as torrefaction atmosphere.

ACKNOWLEDGEMENT

Support from the Ministry of Education Malaysia through HICoE award to CBBR is duly acknowledged. One of the authors (Premchand) would like to greatly acknowledge Universiti Teknologi PETRONAS for financial support under GA scheme to conduct this work.

REFERENCES

Abnisa, F; Arami-Niya, A; Daud, W M; Sahu, J N and Noor, I M (2013). Utilization of oil palm tree residues to produce bio-oil and bio-char via pyrolysis. *Energy Convers. Manag., 76*: 1073-1082.

Agar, D and Wihersaari, M (2012). Bio-coal, torrefied lignocellulosic resources - Key properties for its use in co-firing with fossil coal - Their status. *Biomass Bioenergy, 44*: 107-111.

Aljuboori, A H R (2013). Oil palm biomass residue in Malaysia: Availability and sustainability. *Int. J. Biomass Renew., 2*: 13-18.

Asadullah, M; Rasid, N S; Kadir, S A and Azdarpour, A (2013). Production and detailed characterization of bio-oil from fast pyrolysis of palm kernel shell. *Biomass Bioenergy, 59*: 316-324.

Bilgic, E; Yaman, S; Haykiri-Acma, H and Kucukbayrak, S (2016). Limits of variations on the structure and the fuel characteristics of sunflower seed shell through torrefaction. *Fuel Process. Technol., 144*: 197-202.

Brojolall, N and Surroop, D (2022). Improving fuel characteristics through torrefaction. *Energy, 246*: 123359.

Chai, M; Xie, L; Yu, X; Zhang, X; Yang, Y; Rahman, M M and Cai, J (2021). Poplar wood torrefaction: Kinetics, thermochemistry and implications. *Renew. Sust. Energ. Rev., 143*: 110962.

Chantanumat, Y; Phetwarotai, W; Sangthong, S; Palamanit, A; Abu Bakar, M S; Cheirsilp, B and Phusunti, N (2022). Characterization of bio-oil and biochar from slow pyrolysis of oil palm plantation and palm oil mill wastes. *Biomass Conv. Bioref*. DOI: 10.1007/s13399-021-02291-2.

Eseltine, D; Thanapal, S S; Annamalai, K and Ranjan, D (2013). Torrefaction of woody biomass (Juniper and Mesquite) using inert and non-inert gases. *Fuel, 113*: 379-388.

Financie, R; Moniruzzaman, M and Uemura, Y (2016). Enhanced enzymatic delignification of oil palm biomass with ionic liquid pretreatment. *Biochem. Eng. J., 110*: 1-7.

Hashim, R; Nadhari, W N; Sulaiman, O; Kawamura, F; Hiziroglu, S; Sato, M; Sugimoto, T; Seng, T G and Tanaka, R (2011). Characterization of raw materials and manufactured binderless particleboard from oil palm biomass. *Mater. Des., 32*: 246-254.

Hon, D N S and Shiraishi, N (2001). *Wood and Cellulosic Chemistry*. 2nd edition. Marcel Dekker, New York. p. 296-298, 331.

Howell, A; Stahlfeld, K; Mohammed, A B; Vijlee, S and Belmont, E (2019). Gas independence of *Miscanthus* x *giganteus* torrefied in nitrogen (N_2) and carbon dioxide (CO_2) using calibrated thermogravimetric analysis. *Bioresour. Technol. Rep., 7*: 100238.

Ibrahim, R H; Darvell, L I; Jones, J M and Williams, A (2013). Physicochemical characterisation of torrefied biomass. *J. Anal. Appl. Pyrolysis, 103*: 21-30.

Iovane, P; Donatelli, A and Molino, A (2013). Influence of feeding ratio on steam gasification of palm shells in a rotary kiln pilot plant. Experimental and numerical investigations. *Biomass Bioenergy, 56*: 423-431.

Kanaujia, P K; Sharma, Y; Garg, M; Tripathi, D and Singh, R (2014). Review of analytical strategies in the production and upgrading of bio-oils derived from lignocellulosic biomass. *J. Anal. Appl. Pyrolysis, 105*: 55-74.

Kaniapan, S; Hassan, S; Ya, H; Patma Nesan, K and Azeem, M (2021). The utilisation of palm oil and oil palm residues and the related challenges as a sustainable alternative in biofuel, bioenergy, and transportation sector: A review. *Sustainability, 13(6)*: 3110.

Li, M F; Chen, L X; Li, X; Chen, C Z; Lai, Y C; Xiao, X and Wu, Y Y (2016). Evaluation of the structure and fuel properties of lignocelluloses through carbon dioxide torrefaction. *Energy Conv. Manag., 119*: 463-472.

Li, S X; Chen, C Z; Li, M F and Xiao, X (2018). Torrefaction of corncob to produce charcoal under nitrogen and carbon dioxide atmospheres. *Bioresour. Technol., 249*: 348-353.

Li, X; Lu, Z; Chen, J; Chen, X; Jiang, Y; Jian, J and Yao, S (2021). Effect of oxidative torrefaction on high temperature combustion process of wood sphere. *Fuel, 286*: 119379.

Lv, P; Almeida, G and Perré, P (2015). TGA-FTIR analysis of torrefaction of lignocellulosic components (cellulose, xylan, lignin) in isothermal conditions over a wide range of time durations. *BioResources, 10*: 4239-4251.

Matsunaga, K; Nishi, K; Kamino, Y; Shinmura, T and Kokusho, T (1999). Study on characteristics of bamboo charcoal and bamboo vinegar. *Res. Report Kagoshima Pref. Inst. Indust. Technol., 13*: 23-30.

Na, B I; Kim, Y H; Lim, W S; Lee, S M; Lee, H W and Lee, J W (2013). Torrefaction of oil palm mesocarp fibre and their effect on pelletizing. *Biomass Bioenergy, 52*: 159-165.

Nyakuma, B B; Oladokun, O; Wong, S L and Abdullah, T A T (2021). Torrefaction of oil palm empty fruit bunch pellets: Product yield, distribution and fuel characterisation for enhanced energy recovery. *Biomass Conv. Bioref*. DOI: 10.1007/s13399-020-01185-z.

Onsree, T; Tippayawong, N; Williams, T; McCullough, K; Barrow, E; Pogaku, R and Lauterbach, J (2019). Torrefaction of pelletized corn residues with wet flue gas. *Bioresour. Technol., 285*: 121330.

Poh, P E; Wu, T Y; Lam, W H; Poon, W C and Lim, C S (2020). *Waste Management in the Palm Oil Industry*. Springer. 73 pp.

Premchand; Komiyama, M; Aqsha, A and Uemura, Y (2020). Effect of combustion and nitrogen gas atmospheres on the torrefaction performance of oil palm frond leaves and stems. *IOP Conf. Ser.: Mater. Sci. Eng., 736*: 022020.

Prins, M J; Ptasinski, K J and Janssen, F J (2006). More efficient biomass gasification via torrefaction. *Energy, 31*: 3458-3470.

Rousset, P; Macedo, L; Commandré, J M and Moreira, A (2012). Biomass torrefaction under different oxygen concentrations and its effect on the composition of the solid by-product. *J. Anal. Appl. Pyrolysis, 96*: 86-91.

Sabil, K M; Aziz, M A; Lal, B and Uemura, Y (2013). Effects of torrefaction on the physiochemical properties of oil palm empty fruit bunches, mesocarp fibre and kernel shell. *Biomass Bioenergy, 56*: 351-360.

Shuit, S H; Tan, K T; Lee, K T and Kamaruddin, A (2009). Oil palm biomass as a sustainable energy source: A Malaysian case study. *Energy, 34*: 1225-1235.

Tabakaev, R; Shanenkov, I; Kazakov, A and Zavorin, A (2017). Thermal processing of biomass into high-calorific solid composite fuel. *J. Anal. Appl. Pyrolysis, 124*: 94-102.

Tan, J P; Jahim, J M; Harun, S; Wu, T Y and Mumtaz, T (2016). Utilization of oil palm fronds as a sustainable carbon source in biorefineries. *Intl. J. Hydrog. Energy, 41*: 4896-4906.

Thanapal, S S; Chen, W; Annamalai, K; Carlin, N; Ansley, R J and Ranjan, D (2014). Carbon dioxide torrefaction of woody biomass. *Energy Fuels, 28*: 1147-1157.

Tran, K Q; Trinh, T N and Bach, Q V (2016). Development of a biomass torrefaction process integrated with oxy-fuel combustion. *Bioresour. Technol., 199*: 408-413.

Uemura, Y; Omar, W; Othman, N A; Yusup, S and Tsutsui, T (2013). Torrefaction of oil palm EFB in the presence of oxygen. *Fuel, 103*: 156-160.

Uemura, Y; Saadon, S; Osman, N; Mansor, N and Tanoue, K I (2015). Torrefaction of oil palm kernel shell in the presence of oxygen and carbon dioxide. *Fuel, 144*: 171-179.

Uemura, Y; Sellappah, V; Trinh, T H; Hassan, S and Tanoue, K I (2017). Torrefaction of empty fruit bunches under biomass combustion gas atmosphere. *Bioresour. Technol., 243*: 107-117.

Wertz, J L; Bédué, O and Mercier, J P (2010). *Cellulose Science and Technology*. EPFL Press.

Zhang, J and Zhang, X (2019). 15 - The thermochemical conversion of biomass into biofuels. *Biomass, Biopolymer-based Materials, and Bioenergy* (Verma, D; Fortunati, E; Jain, S; Zhang, X eds.). Woodhead Publishing. p. 327-368.